Agriculture, Ecosystems and Environment 317 (2021) 107484

Contents lists available at ScienceDirect

Agriculture, Ecosystems and Environment

journal homepage: www.elsevier.com/locate/agee

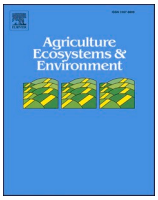

Sediment transport dynamics in small agricultural catchments in a cold climate: A case study from Norway

Hannah Wenng [a,b,*], Robert Barneveld [a], Marianne Bechmann [a], Hannu Marttila [c], Tore Krogstad [b], Eva Skarbøvik [a]

[a] The Norwegian Institute of Bioeconomy Research (NIBIO), P.O. Box 115, 1431 Ås, Norway
[b] Faculty of Environmental Sciences and Natural Resource Management, Norwegian University of Life Science (NMBU), P.O. Box 5003 NMBU, 1432 Ås, Norway
[c] Water, Energy and Environmental Engineering Research Unit, University of Oulu, P.O. Box 8000, FI-90014 University of Oulu, Finland

ARTICLE INFO

Keywords:
Agricultural management
High resolution data
Turbidity
Water discharge
Water quality

ABSTRACT

Increased nutrient and soil losses from agricultural areas into water bodies constitute a global problem. Phosphorus is one of the main nutrients causing eutrophication in surface waters. In arable land, phosphorus losses are closely linked to sediment losses. Therefore, a better understanding of the sediment-runoff processes in agricultural areas is a key to reduce the eutrophication impacts and to implement mitigation measures. The objectives of this study were to identify dominant sediment runoff processes in cultivated grain-dominated catchments in a cold climate. We assessed continuous high-resolution turbidity data, temporal and spatial catchment properties and agricultural management data to describe and get a better understanding of the cause-relationship of sediment transfer in two small agricultural dominated catchments in southern Norway. The concentration-discharge pattern, index of connectivity and agricultural activities were considered with the wider aim to establish a link between field and catchment scale. The results showed that the dominant concentration-discharge pattern was a clockwise concentration-discharge (c-q) hysteresis in both catchments indicating that areas close to or in the stream gave the highest contribution to turbidity. The main driver for turbidity was discharge, though soil water storage capacity, rain intensity and former discharge events also played a role. Intensity of soil tillage and index of connectivity (likelihood of water and particles to be transported to the stream) impacted the c-q hysteresis index. Little vegetation cover and high intensity of soil tillage led to a high hysteresis index, which indicates a quick increase in turbidity following increased discharge. Other links between agricultural management and in stream data were difficult to interpret. The findings of this study provide information about discharge, field operations and vegetational status as drivers for turbidity and about the spatial distribution of sediment sources in two agricultural catchments in a cold climate. The understanding of sediment runoff processes is important, when implementing management actions to combat agricultural emissions to water most efficiently.

1. Introduction

Elevated nutrient and particle concentrations in water bodies as a result of transport from agricultural sites constitute a global problem, leading to deterioration in their ecological status (Bechmann et al., 2008; Giri and Qiu, 2016; Ulén et al., 2007). Phosphorus is one of the main nutrients that cause eutrophication in surface waters and reduces the functioning of a healthy aquatic ecosystem (Álvarez et al., 2017; Schoumans et al., 2014). Areas with marine clay soil, as found in Scandinavia, naturally show a relative high total phosphorus content that is increased by fertilization (Krogstad and Øgaard, 2008). The aim of the European Water Framework Directive (EU, 2000) and other international agreements is to avoid high nutrient loads and control the impact of agriculture and other land use influences on water bodies. Here, the monitoring of small scale catchments can play a key role, because their water quality impacts larger lake and river systems (Bol et al., 2018; Brendel et al., 2019). Typically, the loss of P from agricultural fields is closely associated with particle loss (Ballantine et al.,

* Corresponding author at: The Norwegian Institute of Bioeconomy Research (NIBIO), P.O. Box 115, 1431 Ås, Norway.
E-mail addresses: hannah.wenng@nibio.no (H. Wenng), robert.barneveld@nibio.no (R. Barneveld), marianne.bechmann@nibio.no (M. Bechmann), hannu.marttila@oulu.fi (H. Marttila), tore.krogstad@nmbu.no (T. Krogstad), eva.skarbovik@nibio.no (E. Skarbøvik).

https://doi.org/10.1016/j.agee.2021.107484
Received 22 December 2020; Received in revised form 29 April 2021; Accepted 3 May 2021
Available online 16 May 2021

2009b), which is one reason why it is necessary to monitor suspended sediments (SS) and particle-bound P. Insight into the causes, quantities, and dynamics that characterize phosphorus and suspended sediment fluxes from agriculture is important if effective and efficient measures are to be devised. Sediment monitoring has traditionally been undertaken by grab sampling, continuous sampling with large time lags, and composite sampling on a volume-proportional (flow-weighted) basis. Time-proportional (incl. grab) sampling with low resolution may over time lead to inaccurate estimates of maximum and average concentrations, and it will also fail to detect variation in concentrations. (Leigh et al., 2019; Skarbøvik and Roseth, 2015; Stutter et al., 2017). Provided that the number of subsamples is sufficient, flow-proportional composite sampling will yield more accurate estimates of averages, but the variation will be concealed (Cassidy et al., 2018; Leigh et al., 2019; Villa et al., 2019).

Sensor techniques can show continuous concentrations and therefore provide detailed insight into transport dynamics and the highly variable concentration patterns of particles in streams (Lannergård et al., 2019; Skarbøvik and Roseth, 2015). In particular, continuous high-frequency measuring of turbidity is a useful tool and a surrogate that can be used to detect changes in SS and particle-associated P (Gippel, 1995; Kämäri et al., 2020; Marttila et al., 2013). More frequent data collection may reduce errors in load calculations, as it can capture concentrations during all peak events (Skarbøvik et al., 2012; Valkama and Ruth, 2017). Many different studies have used high-frequency data as a source for process understanding and for estimating nutrients and SS (for example Bieroza and Heathwaite, 2015; Dupas et al., 2015; Fovet et al., 2018; Kämäri et al., 2020; Lannergård et al., 2019; Minella et al., 2008). However, processes have been studied less in sloping landscapes in high latitude climates like Norway (Liu et al., 2019). Cold climate regions are defined by an average air temperature above 10 °C in their warmest month and under 0 °C in their coldest months (Peel et al., 2007). These temperatures, especially in winter, often make it difficult to use sensors the whole year round, and an option for heating is therefore useful (Valkama and Ruth, 2017).

One possible tool for analyzing particle export and discharge is the concentration-discharge (c-q) hysteresis that occurs whenever there is a difference in the relative timing of particle export and discharge during a runoff event (Evans and Davies, 1998). A c-q-approach is important in small catchments (<10 km^2) because small headwater streams are more sensitive to SS and P from local sources than are large catchments. Headwater catchments can provide detailed insight into c-q processes (Bol et al., 2018; Lefrançois et al., 2007). Characteristics such as land use, topography, and annual precipitation patterns (e.g. dry summer, wet autumn) create challenging conditions for mitigating erosion processes. It is particularly challenging to identify, describe and understand the non-point P sources, and sediment and P dynamics at the catchment scale because of spatial heterogeneity and temporal variability (Bol et al., 2018; Haygarth et al., 2012). In addition, the seasonal changes in agricultural management (field operations) and their dependence on precipitation and temperature must be taken into account when dealing with soil and nutrient losses from agricultural catchments (Bieroza and Heathwaite, 2015; Øygarden, 2000). More information is also needed from different locations, as each catchment is unique in its complexity, land-use pressures, catchment size, and predominant processes (Buck et al., 2004; Haygarth et al., 2012; Kämäri et al., 2020). In this context, high-frequency water quantity and quality data analysis, combined with spatial analysis of land use at catchment and field scale, is a powerful tool for understanding dominant transport processes in the terrestrial phase, and for producing better information for management purposes (Barneveld et al., 2019; Keesstra et al., 2019).

We aim to investigate sediment runoff processes in small agricultural catchments in southern Norway that differ in terms of their topography and soil. We analyze high-resolution sensor data on turbidity, combined with spatial and temporal catchment properties and agricultural management factors. The objectives of this research are:

1. To identify the relative importance of near-stream, in-stream and field sources of sediments and particle-bound P.
2. To quantify the (relative) importance of climatic and agronomic drivers that play a role in sediment and particle-bound P loss at catchment scale with respect to seasonality.
3. To establish a causative correlation between agricultural management and turbidity responses in the stream.

The overall aim of this study is to contribute to a better understanding of dominant sediment runoff processes in agricultural headwater catchments with respect to timing and quantity in cold climates.

2. Method and materials

2.1. Study sites

Our case study areas were two small agricultural catchments located in the southeast of Norway (Fig. 1). The Skuterud and Mørdre catchments are part of the Norwegian Agricultural Environmental Monitoring Programme (JOVA) and have been monitored for water quality since the early 1990's. Both catchments are dominated by cereal production, and the soils are tile drained.

Skuterud has a total area of 450 ha and an elevation between 91 and 146 m above sea level. with an average slope gradient of 5.9% (Barneveld et al., 2019) (Table 1). Sixty-two percent of the area is agricultural, of which 80% is under cereal production. The growing season is about 202 days (Wenng et al., 2020). The soils originate from marine deposits, and the main soil textures of the arable land are silty clay, loam, and silty loam (24% sand, 48% silt, 27% clay) (Kværnø and Øygarden, 2006). Skuterud has warm summers (mean temperature 15.6 °C), and winters (mean temperature −2.6 °C) with unreliable snowfall. The annual precipitation is 824 mm and the annual mean temperature is 6.6 °C (Table 1, Wenng et al., 2020).

Mørdre has a total area of 680 ha with an elevation between 130 and 230 m above sea level. (Table 1). Here, 65% of the area is used for agricultural production, of which cereals comprise about 80%. The growing season is about 194 days (Wenng et al., 2020). Mørdre is characterized by ravines, whereas the thalwegs of secondary ravines were artificially levelled in the 1960's to create more suitable land for agricultural production (Barneveld et al., 2019). The average slope in Mørdre is 14.5%. The main soil textures of the arable land are silt, silty clay, and loam (16% sand, 58% silt, 26% clay) (Kværnø and Øygarden, 2006). Mørdre is characterized by a continental climate with warm summers (mean temperature 14.7 °C) and cold winters (mean temperature −4.5 °C). It has higher snow reliability because it is located upcountry and further north (50 km from Skuterud) (Fig. 1). The annual precipitation is 709 mm and the annual mean temperature is 6.1 °C (Wenng et al., 2020).

2.2. Monitoring data

High-resolution turbidity sensors were installed in the outlets of the two catchments. Turbidity was measured every 15 min by the multiparameter sensor MPS-D8 (SEBA Hydrometrie). The detection limit of the sensor was 3210 Nephelometric Turbidity Units (NTUs). For Skuterud, there were two observation periods: the first comprising the years 2015 and 2016, and the second from mid-August 2018 until the end of 2019. In Mørdre, turbidity was measured from mid-August 2018 until the end of 2019. For the monitoring period 2018–2019, the sensors were equipped with a heat wire (Skuterud) and a heat lamp (Mørdre) to prevent the water from freezing, thereby ensuring winter operation. Water level and discharge were monitored continuously using a pressure transducer combined with a Campbell data logger and v-notch dam at the outlet of the catchments. Precipitation was recorded at hourly intervals at local weather stations located in or close to the catchments. In addition, event-based hourly water samples were taken using an ISCO

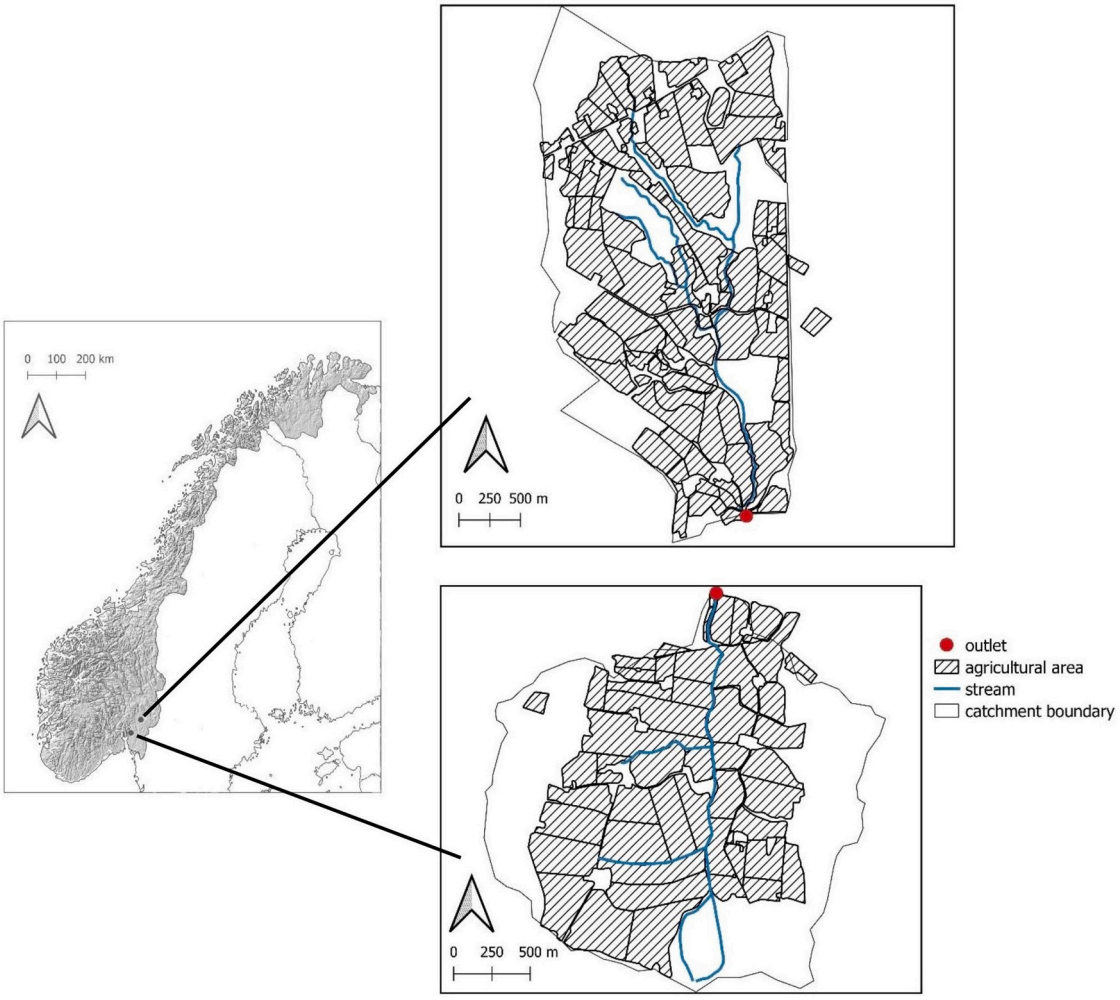

Fig. 1. Locations of the study catchments Mørdre (upper) and Skuterud (bottom) in southeast Norway. The main monitoring station is at the same location as the outlet.

Table 1
Overview of the catchment properties: total area in hectares, land use, main crops, soil texture, elevation, slope, annual mean temperature and precipitation.

Catchment	Total area [ha]	Agricultural land use [%]	Main crops	Soil texture	Elevation range [m.a.s.l.]	Slope [%]	Ann. mean T [°C]	Ann. P [mm]
Skuterud	450	62	cereals	Silty clay, loam, silty loam	91–146	5.9	6.6	824
Mørdre	680	65	cereals	Silt, silty clay, loam	130–230	14.5	6.1	709

portable sampler (Teledyne) to construct calibration curves between turbidity and SS, and between turbidity and total phosphorus (TP). The sampler was usually set up before a rain or snow melting period began, and 24 water samples (500 ml) were taken at hourly intervals for each event. These water samples were analyzed for TP concentration, SS concentration, electrical conductivity (EC), and turbidity in the laboratory. Total phosphorus concentration was determined by oxidative digestion with potassium peroxydisulfate, which is a colorimetric method (Norwegian Standard ISO 11905-1:1997). Suspended sediment concentration was analyzed by filtrating the sample using a glass fiber filter with a pore size of 1.2 μm (Whatman GF-C) and weighing it after one hour of drying at 105 °C. Although this method is standard, it slightly underestimates the SS concentrations, because clay particles are by definition <2 μm and some of the fine particles will pass through the filter pores until they clog. Turbidity measured in NTU was analyzed using the turbidimeter model 2100AN from Hach. Nine events with 221 single water samples were sampled and analyzed for Skuterud, while seven events with 195 single water samples were sampled and analyzed for Mørdre. The high-frequency turbidity data were aggregated from 15-min values to hourly values to correspond to hourly water discharge values.

The JOVA monitoring program also collects land management data. Farmers provide information about crop type, sowing and harvesting dates, the type and date of tillage, yield, fertilizer application date and amount of applied fertilizer (mineral and organic), the type and number of animals, and amount and date of applied pesticides (Bechmann, 2014; Wenng et al., 2020). In our analysis, we linked stream processes to agricultural management data, focusing especially on i) fertilization application and ii) the date and timing of field operations such as sowing, plowing, harrowing, and harvesting.

For information on soil water characteristics, the water storage capacity of the soil was downloaded from the Norwegian data platform (SeNorge.no, 2020) http://www.senorge.no/, an open portal run by the Norwegian Water Resources and Energy Directorate (NVE), the

Norwegian Meteorological Institute (MET), and the Norwegian Mapping Authority. They provide daily data on snow, water, weather, and climate dating back to 1957. These hydrological variables are calculated using the Gridded Water Balance model (GWB) (Beldring et al., 2003).

2.3. Total phosphorus and suspended sediment concentrations and fluxes

A linear relationship between turbidity (hourly sensor data) and TP and SS, respectively, was established from the hourly event-based water samples (Eqs. 1–4). The goodness and significance of the fit were evaluated within a linear regression and the coefficient of determination (R^2). Next, hourly TP and SS concentrations (mg l^{-1}) and fluxes (mg ha^{-1}) for the whole monitoring period 2015–2019 were calculated for each catchment based on Eqs. (1–4).

The SS and TP concentrations of Skuterud and Mørdre were calculated based on:

$$\text{Skuterud: SS concentration} = 0.45*\text{TURB} + (-5{\cdot}1) \quad (1)$$

$$\text{TP concentration} = 0.0009*\text{TURB} + 0.09 \quad (2)$$

$$\text{Mørdre: SS concentration} = 0.39*\text{TURB} + (-2{\cdot}82) \quad (3)$$

$$\text{TP concentration} = 0.0005*\text{TURB} + 2{\cdot}81 \quad (4)$$

2.4. Hysteresis index for turbidity and water discharge

We used a concentration (turbidity) discharge (c-q) hysteresis analysis to analyze processes and sediment sources in the study catchments. Before conducting the hysteresis index analysis, the high-frequency data were checked for outliers and possible measurements errors. All turbidity values above the sensor detection limit (3210 NTU) were deleted, since we assumed that, when these high values occurred in more than one time step in a row, the sensor was most probably blocked by particles or organic matter. Missing values were due to technical problems with the sensor. In total, 4% of the data points were excluded from the analysis.

The start of an event was defined as the onset of precipitation, while the end was defined when precipitation stopped and the discharge was close or similar to that at the start of the event. For each precipitation event, c-q data were plotted and classified into (i) clockwise (cw), (ii) anticlockwise (ac), (iii) eight-shaped (es), or (iv) no hysteresis when an unclear pattern was observed. A clockwise c-q pattern occurs when the peak concentration comes before the peak discharge, whereas, in an anticlockwise c-q pattern, the peak concentration comes after the peak discharge (Williams, 1989). A total of 142 events were identified for Skuterud and 95 events for Mørdre (Table 2). For each hysteresis event, the hysteresis index (HI) created by Lawler et al. (2006) was calculated to classify the events in terms of magnitude and direction and to make them comparable to each other. Subsequently, the Q_{mid} (at 50% of the flow range, Lawler et al., 2006), turbidity for Q_{mid} at the rising limb ($TURB_{RL}$), and turbidity for Q_{mid} at the falling limb ($TURB_{FL}$) were calculated. The HI was determined for the clockwise c-q pattern, where $TURB_{RL} > TURB_{FL}$.

$$HI = (TURB_{RL}/TURB_{FL}) - 1 \quad (5)$$

for the anticlockwise c-q pattern, where $TURB_{RL} < TURB_{FL}$.

$$HI = (-1/(TURB_{RL}/TURB_{FL})) + 1 \quad (6)$$

HI thereby represents both the magnitude of the event and its hysteretic behavior (a positive sign stands for clockwise and a negative sign for anticlockwise) (Lawler et al., 2006). In addition to the HI, we calculated the rise in the discharge and turbidity within the first hour of the event and the increase in the discharge and turbidity at the steepest point of the rising limb to get an indication of how quickly the systems

Table 2
Characteristics of the events for Skuterud (Sku) and Mørdre (Mør) with number and types of patterns, average, minimum and maximum discharge (Q) values, average, maximum and minimum turbidity, mean and maximum hysteresis index (HI), average rain intensity, water storage capacity, mean and median crop factor and the mean normalized connectivity index and the timing of the Q peak.

	No. of events	No. and types of pattern	Q [$m^3 s^{-1}$]			Turbidity [NTU]			HI [-]		Rain intensity [mm h^{-1}]	Water storage capacity of soil [mm]			Crop factor [-]		Connectivity index [-]		Timing Qmax [h]	
			Min	Mean	Max	Min	Mean	Max	Mean	Max	Mean	Max	Mean	Max	Mean	Median	Mean		Mean	
Sku	142	97 cw, 9 ac, 11 es, 25 no pattern	0.07	0.2	0.45	29	91	339	1.94	14.9	0.47	25	120	194	0.51	0.50	0.68		12	
Mør	95	63 cw, 1 ac, 1 es, 31 no pattern	0.11	0.25	0.47	93	292	904	2.23	7.3	0.3	12	79	168	0.50	0.46	0.39		15	

reacted.

2.5. Crop factor and hydrological connectivity index

A crop factor (C, dimensionless) was calculated for the years 2015, 2016, 2018, and 2019 for each agricultural unit in the catchment (Barneveld et al., 2019). The crop factor represents the protection of vegetation against particle loss. A value of 1 represents no vegetation combined with autumn tillage, while a value of 0.01 represents fully developed crop vegetation in the fields (following Barneveld et al., 2019). It gives an indication of the impact of agricultural activities and crop growth on particulate sediment transport through surface and subsurface pathways. Daily C factors were calculated for each field. Each field operation was assigned initial and final C values. The C values are then allowed to develop over time, depending on their operation. If the operation is sowing or planting, C values decrease with assumed vegetative growth and according to the daily temperature. All other operations are followed by a gradual decrease in the C value over time. Changes in field operations and vegetation cover during an agricultural year will also impact the hydrological and sediment connectivity of water and particles to the stream. We calculated a connectivity index based on the procedure in Borselli et al. (2008). The Borselli index of connectivity (IC, dimensionless) expresses the spatially distributed probability that water and sediments will be transported from a location to a predefined sink. The index has an upstream and a downstream component. The upstream component consists of the contributing area and its average value for slope steepness and a weighting factor that describes the soil surface's ability to convey matter. The downstream component is the length of the path to the sink, divided by steepness and the weighting factor. In this study, the C factor values were used as the weighting factor for the index of connectivity. This combination of IC and C is expected to represent the seasonal effect of agronomic activity on the catchment's connectivity. We also calculated a version including the tile drains, but it did not produce any different results for the IC at catchment scale.

2.6. Statistical analysis

Two datasets, the event dataset (the event-based hourly water grab sampling data) and the hourly sensor dataset formed from previously described data, served as the basis for the statistical analysis. The event dataset consisted of information about the events' mean event turbidity ($TURB_{mean}$), maximum and minimum event turbidity ($TURB_{max}$, $TURB_{min}$), sum of precipitation, rain intensity, HI, and TP and SS concentration and fluxes, the mean event discharge (Q_{mean}), maximum and minimum event discharge (Q_{max}, Q_{min}), event length in hours, crop factor (C), and connectivity index (IC), water storage capacity of the soil (wsc), and the hourly increase in discharge and turbidity at the beginning and at the steepest point of the rising limb during the specific events. The hourly dataset (Fig. 2) contained the total hourly turbidity data and the corresponding calculated TP and SS concentrations and fluxes for the whole monitoring period (2015–2019). Analyses of variance (Kruskal–Wallis) and post-hoc tests (Wilcoxon-Mann-Whitney) were carried out to compare the characteristics (runoff and water quality) of the two catchments and to determine the seasonal differences. When comparing the two catchments, the monitoring data from Skuterud for 2015 and 2016 were excluded to ensure the same timeframe for both sites. When analyzing the catchment data individually, the years 2015 and 2016 were included for Skuterud. First, a Spearman correlation was used to link the single process parameters to each other. Second, multivariate regressions were compiled to consider the intercorrelation between the explanatory variables. The dependent variables were Q_{mean}, Q_{max}, $TURB_{mean}$, and $TURB_{max}$. Explanatory variables were event Q_{mean} and Q_{max} (for turbidity), total precipitation per event, rain intensity per event, water storage capacity, crop factor, and index of connectivity. Seasons used in this study were defined as winter (December–February), spring (March–May), summer (June–August), and autumn (September–November). A 95% confidence interval and 5% significance level were set throughout the statistical analysis, which was carried out in R version 3.5.2.

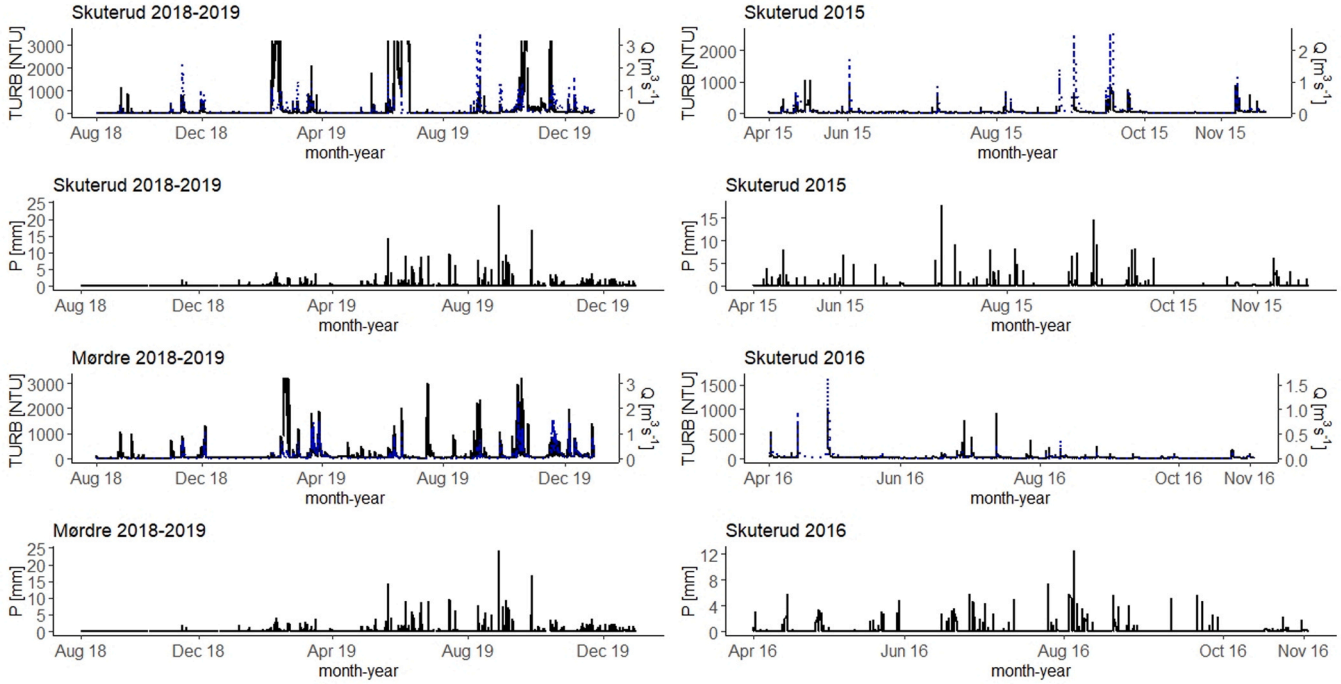

Fig. 2. Time series (hourly data measured by the sensor) of turbidity (TURB), discharge (Q, marked in dashed blue) and precipitation (P) for the periods 2015, 2016, 2018–2019 for the Skuterud catchment and 2018–2019 for the Mørdre catchment. (For interpretation of the references to color in this figure legend, the reader is referred to the web version of this article.)

3. Results

3.1. Phosphorus and suspended sediment concentrations related to turbidity

The results of the linear regressions between turbidity and TP and SS, respectively, showed that turbidity is a good proxy for concentrations of both TP and SS in the two studied catchments. In total, five data points of 221 turned out to be outliers for the Skuterud catchment and were excluded (Fig. 3). Here, a large discrepancy between laboratory values and what was measured in the field led to the assumption that there were errors in the measurements for these five data points in either the laboratory or the field. In Mørdre, one outlier was detected and excluded for the same reason as in Skuterud.

For Skuterud, a good fit was found between SS concentration and turbidity, with a significant R^2 of 0.75, and a significant positive correlation between TP and turbidity ($R^2 = 0.63$) (Fig. 3a, b). For Mørdre (Fig. 3), the linear regression showed a significant relationship between concentration of SS and turbidity, and TP and turbidity (Fig. 3c, d R^2 is 0.85 and 0.65, respectively).

3.2. Seasonal differences

Runoff was highest during autumn 2019 for both catchments, in Skuterud, 44%, and in Mørdre, 41% of the annual runoff. Spring and winter runoff also play an important role in the yearly runoff. In Skuterud, 30% of the runoff occurred during the winter and 18% in the spring. In Mørdre in 2019, runoff during spring and winter constituted 28% and 25% of annual runoff. Summer plays a minor role due to less rainfall. These patterns were found throughout the monitoring period (Fig. 4). The datasets resulted in significant seasonal differences ($p = 0.0$) in discharge, with autumn being the dominant season in Skuterud and spring the dominant season in Mørdre (Fig. 4).

In Skuterud in 2019, the SS loads were highest in autumn and winter, with 53% and 32% of the total annual load, respectively. Turbidity showed a similar pattern. Spring and summer 2019 accounted for 7% and 8% of the annual SS load. The distribution is the same for the whole dataset (Fig. 4). In Mørdre, 43% of the annual SS load in 2019 occurred in the autumn and 26% in winter and spring. Turbidity followed a similar pattern (Fig. 4). Both autumn and winter play a major role in particle loss in Skuterud and Mørdre (Fig. 4). Spring seems to be slightly more dominant in Mørdre than in Skuterud when both discharge and turbidity are considered.

All seasons in both catchments were dominated by a clockwise HI

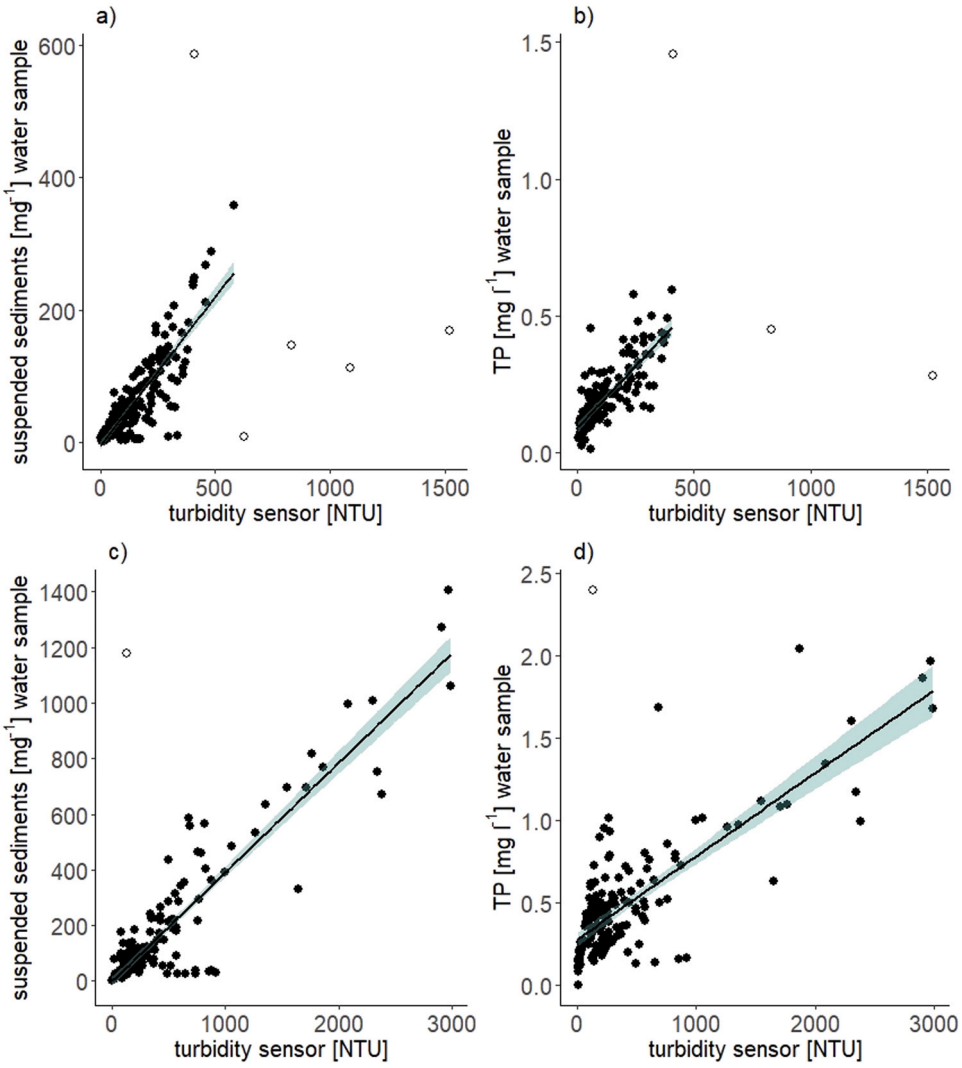

Fig. 3. Relation between suspended sediments and total phosphorus from the hourly water samples and turbidity measured by the sensor for Skuterud a), b) and Mørdre c), d). The unfilled data points were outliers and taken out from the analysis. Please note the different axis scales.

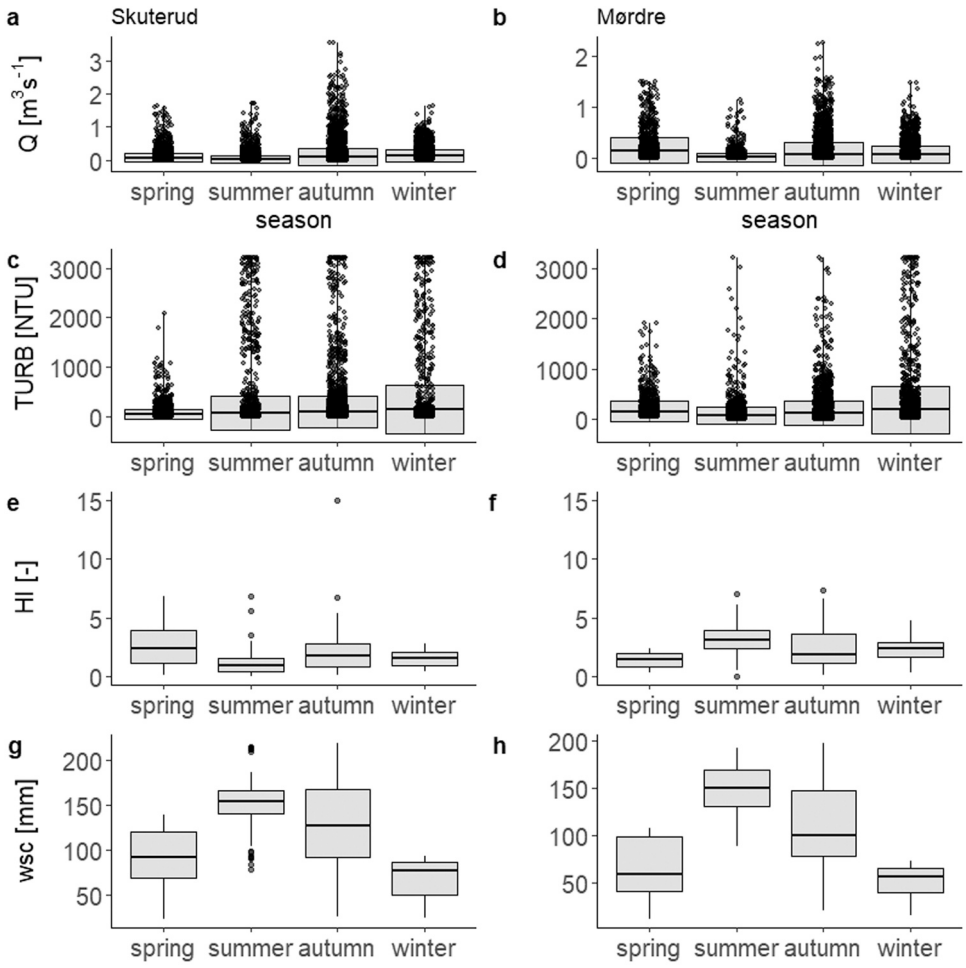

Fig. 4. Boxplots across the seasons for Skuterud (left column, period 2015, 2016, 2018–2019) and Mørdre (right column, period 2018–2019); a), b) hourly runoff data; c), d) hourly turbidity data; e), f) hysteresis index (HI); g), h) average daily soil water storage capacity (wsc).

(turbidity-water discharge pattern and its magnitude). The magnitude was higher in spring and autumn than in summer (Fig. 4), which means that both discharge and turbidity are higher in autumn and spring than in summer. For Mørdre, the tendency towards a corresponding seasonal difference in HI between spring and summer ($p = 0.061$), with the highest magnitude in summer (Fig. 4), might be due to a shorter

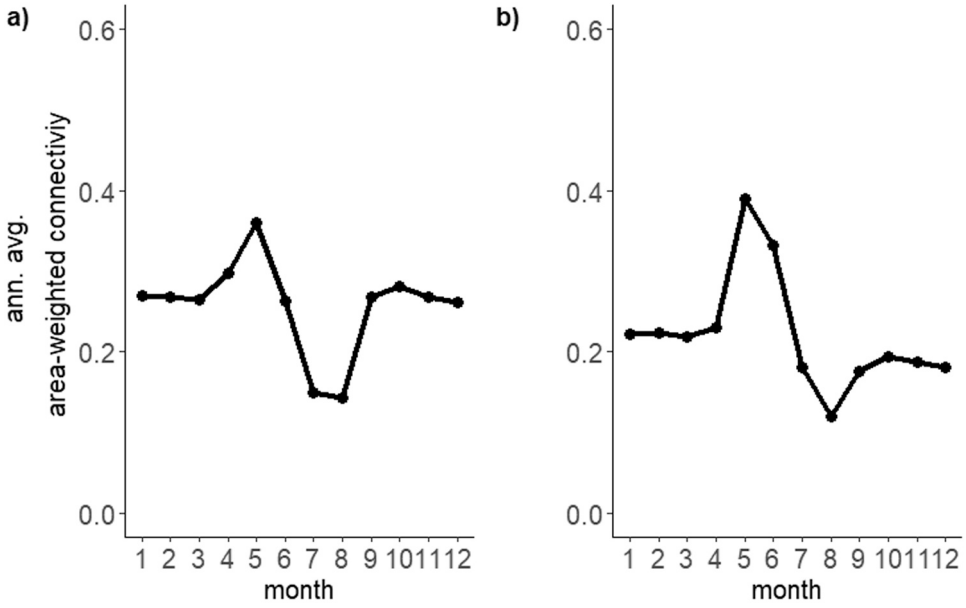

Fig. 5. Normalized average monthly area-weighted index of connectivity over the whole JOVA monitoring period (1990–2019) for Skuterud a) and Mørdre b).

monitoring period and therefore few data for spring.

Other variables, such as the water storage capacity of the soil and the connectivity index, also showed seasonal variations (Figs. 4, 5). Water storage capacity (Fig. 4) showed a clear seasonal pattern, with the lowest storage capacity in winter (wet conditions, frozen soil) and highest in summer (dry conditions). Annual average, area-weighted connectivity calculated for the whole JOVA monitoring period (1990–2019) also showed a seasonal pattern (Fig. 5). The index of connectivity is highest during May and during autumn, followed by winter, due to a low crop factor when fields are only covered with sparse vegetation and when a lot of field operations are taking place, such as ploughing, seedbed preparation, and sowing. The highest crop factor, and hence lowest connectivity, was in summer. During May, autumn and winter, the soil surface conditions are more conducive to particle transport, and the probability of water or particles being transported to the channel is higher in these seasons than in summer conditions. Here, the index of connectivity was lowest when fully developed vegetation cover was found on the fields (Fig. 5).

3.3. Runoff and turbidity

As noted above, the c-q patterns of the events were dominated by clockwise hysteresis (positive HI), despite the differences in topography and soil characteristics (Table 2), meaning that turbidity in general peaked before the discharge peak. Significant differences between the two catchments could be seen for the mean turbidity values and for maximum turbidity during the events ($p = 0.0$), with higher values for Mørdre than for Skuterud (Table 2). The analysis of hourly turbidity for the whole period showed a similar picture, with higher turbidity for Mørdre than for Skuterud (Fig. 2). Neither mean nor maximum event discharge (Table 2), nor the average hourly discharge, varied between the catchments. The calculated HI for each event did not differ significantly between the two catchments, although Mørdre had a higher average HI value, meaning that the events had a larger magnitude.

There was a significant positive relationship between discharge and turbidity in both catchments, which is not only valid for the single events (Table 3), but also for the hourly sensor data (Skuterud $R^2 = 0.76$, Mørdre $R^2 = 0.75$, data not shown). Thus, turbidity increases with increasing discharge, as do TP and SS concentrations and fluxes.

Skuterud was found to have a significantly higher median crop factor than Mørdre (Table 2). This is due to more autumn tillage in Skuterud than in Mørdre. A comparison of the connectivity index resulted in significantly higher connectivity in Skuterud than in Mørdre, which fits with the result that, in Mørdre, the events lasted longer and the discharge peak took longer to appear after the event began (Table 2).

The relative importance resulting from the multivariate regression showed that, in both catchments, precipitation and water storage capacity largely explained the variation in event Q_{mean} (Table 4). Soil water storage capacity plays a major role for Q_{mean} in both catchments, because it determines the baseflow. Connectivity played a minor role in both catchments. The maximum event Q_{max} showed a similar pattern as the event Q_{mean} in Skuterud and in Mørdre (Table 4). The Q_{max} was the main explanatory variable for mean event $TURB_{mean}$ and maximum event $TURB_{max}$ in both catchments (Table 5). Hence, Q_{max} has the energy to transport the particles.

Table 3
Significant correlations (in bolt) between event parameters mean and maximum discharge (Q_{mean}, Q_{max} [m^3s^{-1}]), mean turbidity ($TURB_{mean}$ [NTU]), rain intensity [mm hr^{-1}], water storage capacity [mm], crop factor [-] and connectivity index [-].

	Skuterud			Mørdre		
	Q_{mean}	$TURB_{mean}$	HI	Q_{mean}	$TURB_{mean}$	HI
Q_{mean}		**0.66**	**0.54**		**0.53**	0.21
Q_{max}		**0.81**	**0.64**		**0.69**	**0.33**
Rain intensity	**0.28**	**0.4**	0.14	**0.26**	**0.63**	0.21
Water storage capacity	**-0.71**	**-0.44**	**-0.25**	**-0.7**	-0.18	0.13
Crop factor	0.11	-0.03	**0.33**	**-0.24**	-0.06	**0.28**
Connectivity index	**0.2**	0.001	**0.4**	-0.28	-0.1	**0.28**

3.4. Rain intensity, water storage capacity of the soil, crop factor, and connectivity

Rain intensity showed a significant positive correlation with mean event turbidity for Skuterud ($R^2 = 0.40$) and Mørdre ($R^2 = 0.63$) (Table 3). The result of the multivariate regression showed that rain intensity explains 21% of the mean event $TURB_{mean}$ in Skuterud and 36% in Mørdre (Table 5). Furthermore, the water storage capacity of the soil correlated with mean event Q_{mean} and mean event $TURB_{mean}$. The storage capacity showed a significant negative correlation with discharge in both catchments, which means that higher storage capacity can result in less discharge (Table 3). The same explanatory power was shown in the multivariate regression (Table 4). The event $TURB_{mean}$ had a significant negative correlation with water storage capacity in Skuterud; hence, the less available storage capacity, the more surface runoff and more particle transport (Table 3). In Mørdre, the correlation was also negative, but not significant (Table 3). The multivariate regression showed that the water storage capacity of the soil explained 4–13% of the variation in mean and maximum event turbidity for Skuterud and Mørdre (Table 5).

The crop factor (combined field activity and crop cover) correlated significantly positively with the HI in Skuterud ($R^2 = 0.33$) and Mørdre ($R^2 = 0.28$) (Table 3). This means that little vegetation cover combined with soil tillage lead to a higher HI. Moreover, the connectivity index correlated significantly positively with the HI index for Skuterud ($R^2 = 0.4$) and Mørdre ($R^2 = 0.28$) (Table 3). The additional information on distance from field to stream and the upstream area contribution did not add to the explanation of HI in Mørdre.

Any further direct linkage between the crop factor and index of connectivity with other parameters such as discharge and $TURB_{mean}$ was limited (Table 3). Although the connectivity index correlated significantly positively with mean event Q_{mean} ($R^2 = 0.2$) in Skuterud, such a pattern was not seen in Mørdre, probably due to a smaller dataset. No significant correlation was found between Q_{max} and crop factor and index of connectivity in either catchment.

The results of the multivariate regression showed that connectivity only contributed a little to explaining the variation in Q_{mean}, Q_{max} (Table 4), $TURB_{mean}$, and $TURB_{max}$ (Table 5) in Skuterud and Mørdre. The crop factor did not improve the multivariate regression. Furthermore, there was no correlation between the connectivity index and the timing of the turbidity peak, nor between the connectivity index and the steepness of the increase in discharge and turbidity at the beginning of an event and the steepest point of the rising limb of hysteresis (data not shown).

3.5. Pre-event conditions

Previous runoff events determine the moisture content of the soil and the availability of particles from both surrounding fields and channel to be eroded and transported. We calculated a ratio between the Q_{max} of the previous event and the next event ($Q_{max\text{-}j}/Q_{max}$) and correlated it with maximum turbidity of the latter event (Fig. 6). It turned out that high ratios (pre-event runoff peak > event peak) were linked to rather small turbidity values at the event peak (Fig. 6). This indicates that large pre-events flush most of the easily available stored particles, and that less sediment will be available in following events. Small ratios (pre-event peak < event peak) are linked to high turbidity values (Fig. 6). Hence, small pre-events leave more material that can be transported in the next event.

Table 4
Multivariate regression for event mean (Q_{mean} [$m^3 s^{-1}$]) and maximum (Q_{max} [$m^3 s^{-1}$]) discharge, showing the total explanation of the model and the partial explanation of sum of precipitation [mm], water storage capacity [mm] and connectivity index [-]. *Significant effect

	Skuterud				Mørdre			
	Total 46% p = 0.0	Q_{mean}	Total 48% p = 0.0	Q_{max}	Total 46% p = 0.0	Q_{mean}	Total 56% p = 0.0	Q_{max}
Explanatory variables								
Sum precipitation		41%*		66%*		23%*		53%*
Water storage capacity		57%*		32%*		65%*		41%*
Connectivity index		2%		1%		11%		6%

Table 5
Multivariate regression for mean ($TURB_{mean}$) and maximum ($TURB_{max}$) event turbidity. Numbers show how much of the variation is explained with all variables and how much each variable explains (*significant effect).

	Skuterud				Mørdre			
	Total 66% p = 0.0	$TURB_{mean}$	Total 30% p = 0.0	$TURB_{max}$	Total 64% p = 0.0	$TURB_{mean}$	Total 51% p = 0.0	$TURB_{max}$
Explanatory variables								
Qmax		65%*		79%*		59%*		71%*
Rain intensity		21% (p = 0.09)		13%		36%*		16%
Water storage capacity		13%*		4%		4%		12%*
Connectivity index		1%		5%		1%		2%

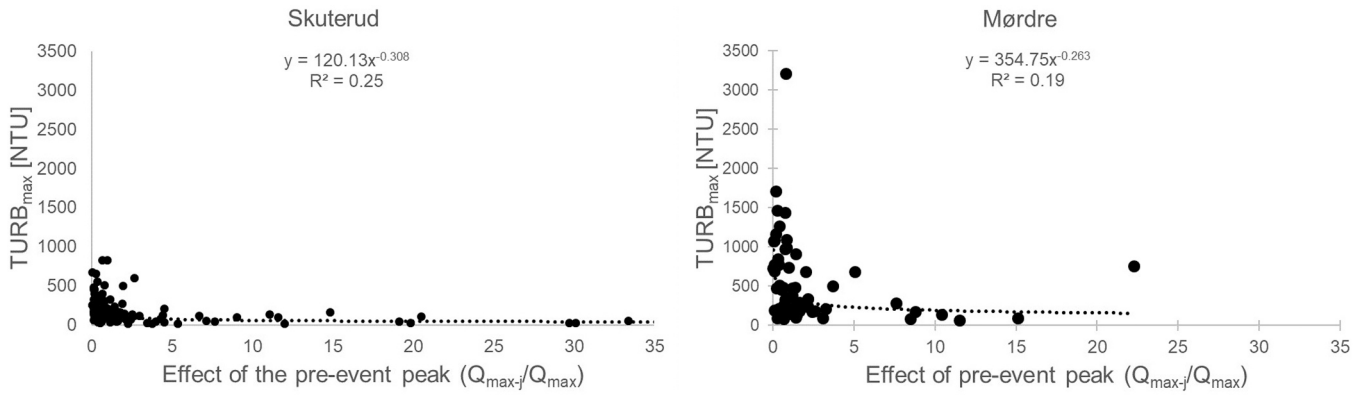

Fig. 6. Relationship of ratio between Q_{max-j} of the previous event and the next event Q_{max} (Q_{max-j}/Q_{max}) and maximum event turbidity ($TURB_{max}$) for Skuterud and Mørdre.

4. Discussion

4.1. Concentration – discharge pattern

The dominant c-q pattern in both catchments was clockwise (Fig. 7). This fast transport of SS and TP is typical of small-scale catchments (Heidel, 1956). Other studies have also found that a clockwise c-q pattern for SS and TP dominates in agricultural headwater catchments (Keesstra et al., 2019; Outram et al., 2016; Rose et al., 2018). Furthermore, catchments dominated by clay soils, characterized by a preferential flow through macropores and tile drains and by overland flow, lead to a fast response of SS and TP (Bieroza et al., 2019; Ulén et al., 2018). Both catchments are tile-drained, which may explain the dominance of the clockwise c-q pattern. On average, Mørdre had higher mean turbidity values in the events and over the whole monitoring period (hourly sensor dataset) (Fig. 2), which can be explained by higher erodibility due to steeper channel slopes and hilly topography. According to Barneveld et al. (2019), gully erosion contributes to 66% of the total soil loss in Mørdre and to only half as much in Skuterud. Moreover, channel bed dynamics, stream bank erosion, and remobilization of particles may also be impacts that are important in Mørdre, where the main channel is wider (5–10 m) and has longer slopes than in Skuterud (<5 m channel width). In addition, meandering is more active in Mørdre than in Skuterud (Barneveld et al., 2019).

In our study sites, the good fit between turbidity, SS, and TP shows that turbidity can be used as a substitute for SS and TP. This is consistent with previous observations, including Norwegian, Swedish, and Finnish agricultural catchments (Kämäri et al., 2020; Sandström et al., 2020; Skarbøvik and Roseth, 2015; Villa et al., 2019). Phosphorus is mainly bound to soil particles (Walling et al., 1997) and it is especially positively correlated with small particles such as clay, which have a larger relative surface area (Ballantine et al., 2009b; Kleinman et al., 2011; Sandström et al., 2020). Skuterud and Mørdre both have soils with a high clay and silt content, which influences the SS and TP concentrations in the stream.

The relationship between TP concentration and turbidity shows a larger slope in Skuterud than in Mørdre, which means that, with the same level of turbidity, Skuterud has higher TP concentrations than Mørdre (Fig. 3). This is consistent with the results from the annual TP loss analysis, which show higher TP concentrations in Skuterud than in Mørdre. This was also found by Bechmann et al. (2008). Furthermore, the TP–turbidity relationships show that, even when turbidity is zero,

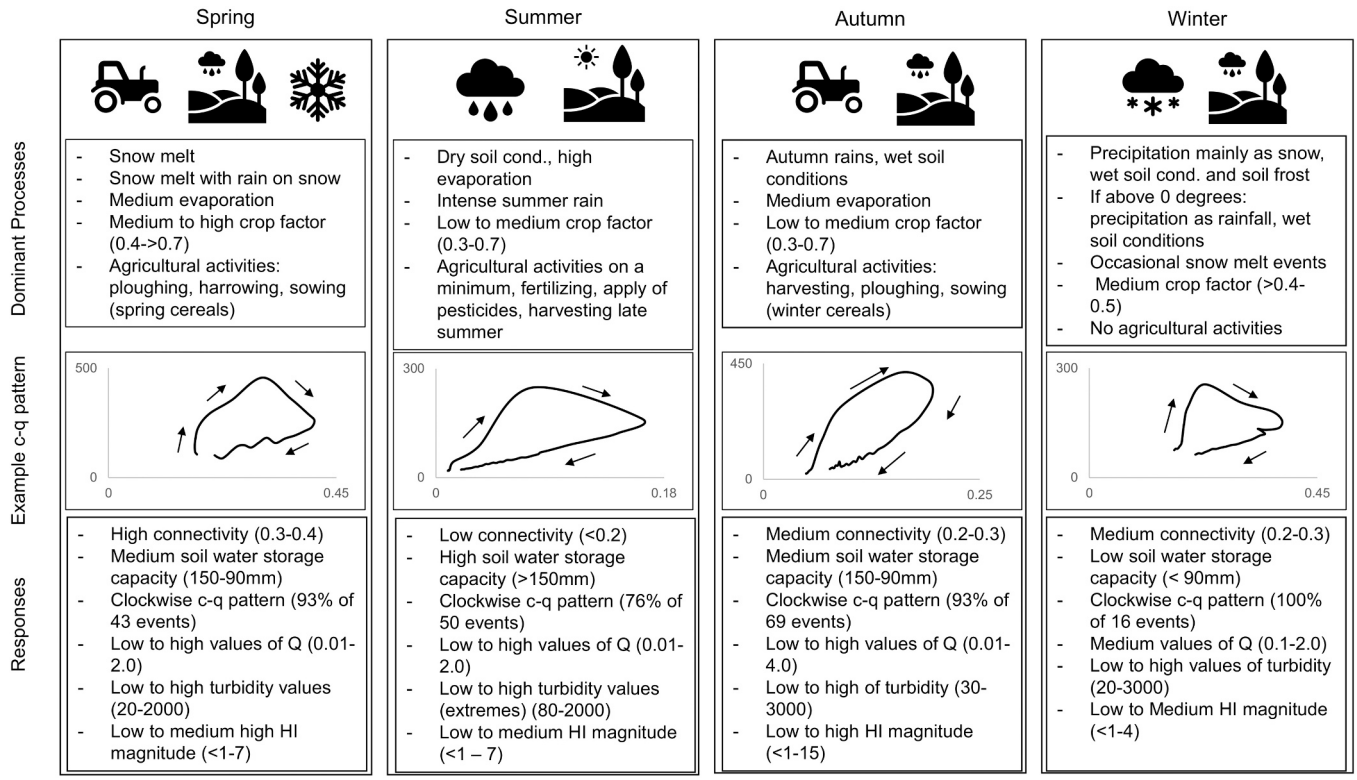

Fig. 7. Conceptual model for the seasonal dominant processes and main responses based on the analyzed data and showing examples for a concentration-discharge hysteresis patterns.

there is still P transport that is not particle-bound. Withers et al. (2012) showed that the contribution from scattered dwellings in Mørdre was 51 kg P yr^{-1}, whereas in Skuterud it was only 7.4 kg P yr^{-1}. This must be taken into account if the P concentration in the suspended sediments is to be estimated. Especially in the case of low turbidity, the TP will overestimate the content of P in soil particles. However, the value of high-frequency turbidity data is that they contribute to understanding runoff processes of SS and TP, and turbidity is a reliable proxy for SS and TP during high runoff events.

4.2. *Future perspective: climate change*

Our results show that discharge is the main driver of turbidity (explains more than 50% of the variation), and hence also of SS and TP, in our sites (Table 5). We observed that rain intensity influenced the average event turbidity values (Tables 3, 5). This is important because the number of intense local rain events in the Nordic countries is expected to increase (Hanssen-Bauer et al., 2015), which entails a risk of higher turbidity values in agricultural streams.

For Norway, the change in the total annual discharge is predicted to be small, whereas seasonal changes are expected to be high (Hanssen--Bauer et al., 2015). Moreover, it is assumed that winter discharge will increase, that winters will be warmer, and that water runoff will decrease in summer. Skuterud and Mørdre showed an increase in the mean annual temperature, while Skuterud also showed an increase in annual discharge during the period 1994–2017 (Wenng et al., 2020). These changes might contribute to higher sediment concentrations and sediment fluxes in the future (Fig. 7), especially in seasons when the soil is not covered by plants and therefore more exposed to erosion (Ulén et al., 2010). Autumn ploughing will leave the soil bare during this period of higher erosion risk. This is also important for extreme events, because the maximum turbidity values are highly correlated with maximum discharge. The winter of 2019 contributed to rather high turbidity values (Skuterud 27% and Mørdre 35% of annual turbidity) due to mild conditions with relatively more rain than snow compared to the long-term average. At lower temperatures, decreasing soil hydraulic conductivity weakens the ability of soil to transport water and leads to increased surface runoff and particle loss (Gao and Shao, 2015; Wu et al., 2018). Spring and autumn have been known as seasons for soil loss in the Nordic countries (Deelstra, 2015), due to snow melt periods combined with rain early in the year and wet periods after harvesting in autumn. The winter season also plays an important role in particle and nutrient runoff in the Nordic countries, alternating between freezing and thawing and, consequently, snowmelt (Øygarden, 2000). There is still a high risk of soil loss in the spring season in Mørdre (Figs. 2, 4), where the average snowfall is higher than in Skuterud due to differences in climate regions. However, even today, winters can contribute to severe erosion and sediment transport events if there is no permanent snow cover (Øygarden, 2003; Skøien et al., 2012). The data showed that, in winter and spring, the water storage capacity of the soil was very low (Fig. 4), due to frozen or wet conditions. This means that the capacity of the soil to take up water is very limited in these seasons. Hence, stubble, cover crops, and no autumn tillage play an even more important role in protecting freshwater systems in agricultural areas during the relatively long non-growing season in the north (Liu et al., 2019; Skøien et al., 2012). High levels of turbidity can also occur during rainstorms in summer (Skuterud; Fig. 4), even though the fields have a fully developed vegetation cover. A Canadian study also found peaks in discharge linked to high TP concentrations during summer (Casson et al., 2019). However, although turbidity and concentrations of SS may be high during summer, discharge is low, and therefore the total loss of particles is low compared to other seasons (Fig. 7). A higher frequency of extreme precipitation during summer is predicted in the Nordic countries, which could also increase the number of discharge and nutrient peaks during the summer season (Hanssen-Bauer et al., 2015; Wiréhn, 2018). Factors controlling turbidity differ with the seasons (Fig. 7), as reflected in, for example, the seasonality of temperature, water storage capacity of the soil, the annual average connectivity, and the crop factor (Figs. 4, 5).

Lefrançois et al. (2007) found seasonal variation in SS due to the evolution of sediment supply and deposited and stored sediment during a hydrological year. Although we have no direct measurements from our study sites, we could expect similar behavior with stored sediments (Ballantine et al., 2009b). This is consistent with the suggestion by Casson et al. (2019) that drivers of P dynamics also vary by season, as do patterns of nutrient loss (Liu et al., 2019).

4.3. Linking field activities and the index of connectivity to turbidity response

In this study, the crop factor could be directly linked to the HI, and, hence, to a combination of discharge and turbidity. Both the vegetation and agricultural management (tilled, not tilled etc.) have an impact on water runoff and particle (and therefore TP) loss. A well-developed vegetation cover affects the runoff through interception, better infiltration, and soil protection (Blankenberg and Skarbøvik, 2020; Stutter et al., 2019), whereas soil cultivation can lead to loose material being available for erosion (Bechmann et al., 2008; Ulén et al., 2007). A correlation was also seen between the index of connectivity and the HI. Bracken et al. (2013) also showed that connectivity plays an important role in runoff processes. However, we found that the connectivity index only had limited explanatory power for the mean event discharge and turbidity. The difficulties in linking the connectivity index to discharge and turbidity could be due to catchment size. The catchments are small, and the distances from field to (higher order) stream are relatively short compared to distances in larger catchments, which may explain why the distance from field to stream is of less consequence in small catchments.

On field scale, the effects of field operations and vegetation cover can clearly be seen (Skøien et al., 2012). At catchment scale, there is a heterogeneity of field operations. Not all farmers perform the same operations at the same time on their fields. Hence, a signal from single-field operation is difficult to detect directly in the channel. Other internal catchment variabilities may also play a role, such as microtopography and heterogeneity in vegetation development (Luo et al., 2018). Direct detection of the impact of field operation is often also a matter of timing in combination with precipitation. Water and particles are not always transported to the stream or outlet during one and the same event (Ballantine et al., 2009a, 2009b). They may be temporarily stored in fields, buffer zones, or upper stream channel systems before finally being transported to the stream outlet. Nevertheless, some studies show that, for example, autumn tillage influences particle loss and water quality (Farkas et al., 2013; Rankinen et al., 2015).

Moreover, Haygarth et al. (2012) suggest that, if the impact on a stream can hardly be seen, this might be due to the sampling frequency. Even with high-frequency data, however, not all single sources, processes, and pathways can be documented due to the complexity on the catchment scale and the influence of variation in time and space on runoff generation. It is indeed difficult to observe management practices in stream data, since nutrient transfer in agricultural catchments is not just caused by a single process (management), but by several processes which are not always active. Nevertheless, small headwater catchments provide the conditions required to observe this link (e.g., Kyllmar et al., 2006 and as shown here with the crop factor, the connectivity index and HI). Water quality concerns about sediments and P apply on the catchment scale rather than on farm or individual field scale (Sharpley et al., 2009). Small catchments can enable us to discover these links and to better explain and understand dominant processes during different seasons with different management options, and make it possible to take a more integrative approach to cover the complexity of processes (Bol et al., 2018). They are a key influence on the environmental state and nutrient levels of larger lakes and catchments, and are therefore of great importance, especially when they are well monitored (Bol et al., 2018). These issues are also important for farmers and land managers, when it comes to the question of which mitigation measures to choose and where to locate them in the catchment.

5. Conclusion

Studying high-resolution data from two agricultural catchments has led to the following conclusions:

1. The clockwise c-q pattern was dominant in both catchments (although they differ in topography and soil type), which suggests particles eroded from banks and channels and particles that are quickly transported from fields. The catchment (Mørdre) with the highest turbidity also had the highest HI. This indicates that the sediment sources were closer to the stream in this catchment and of importance to the particle loss.
2. We found that the main driver of turbidity was discharge and variation in it. However, in the field, it was noted that soil water storage capacity influenced discharge and turbidity, while increased rain intensity led to higher in-stream turbidity values. Furthermore, turbidity was shown to depend on previous discharge events, with lower turbidity than normal occurring after a high pre-event peak, probably because the amount of readily available soil and sediment material had been depleted.

   Autumn and spring were the dominant seasons for discharge, due to autumn rainfall, snowmelt and rainfall periods in spring. Spring, autumn, and winter were important to turbidity, in spring and autumn due to high field activities, such as ploughing, in combination with rainfall. High turbidity during winter was due to non-permanent snow cover and rain.
3. Agricultural management (crop factor) and the index of connectivity influenced the c-q hysteresis index. A high crop factor (little vegetation cover and high soil tillage) and a high index of connectivity resulted in a large hysteresis index, indicating large event-triggered sediment transport. No other direct connections were detected between agricultural management and response in the streams.

Linking drivers directly to a response in the stream is challenging due to the nature of the catchments. Catchment heterogeneity and complexity buffers the effect of a direct response. Moreover, hydrological drivers have a dominating influence on discharge and turbidity, masking the effects of other factors in the catchment. High-resolution turbidity data are valuable for describing and understanding processes at catchment scale, but are also somewhat limited. The findings in this study provides information about drivers of turbidity, and therefore of soil, sediment, and phosphorus losses from agricultural catchments. They also offers insights that can help with the selection of the most appropriate mitigation measures in different seasons. This insight into processes should also be applicable in other cold-climate regions with comparable conditions. Moreover, our study demonstrates a method for analyzing high-frequency datasets that could be followed up by studies in regions with different soil, climate, and hydrological conditions, hence improving the planning of site-specific and seasonally adapted environmental mitigation measures.

Funding

The research project was supported by the Nordic Centre of Excellence BIOWATER, funded by NordForsk under Project No. 82263. The Ph.D. scholarship for Hannah Wenng is funded by the Research Council of Norway. The Norwegian Agricultural Environmental Monitoring Program (JOVA) is funded by the Ministry of Agriculture and Food and run by the Norwegian Institute for Bioeconomy Research (NIBIO). Open Access funding provided by NIBIO.

Declaration of Competing Interest

The authors declare that they have no known competing financial interests or personal relationships that could have appeared to influence the work reported in this paper.

References

Álvarez, X., Valero, E., Santos, R.M.B., Varandas, S.G.P., Sanches Fernandes, L.F., Pacheco, F.A.L., 2017. Anthropogenic nutrients and eutrophication in mutiple land use and watersheds: Best management practices and policies for the protection of water resources. Land Use Policy 69. https://doi.org/10.1016/j.landusepol.2017.08.028.

Ballantine, D., Walling, D.E., Collins, A.L., Leeks, G.J.L., 2009a. The content and storage of phosphorus in fine-grained channel bed sediment in contrasting lowland agricultural catchments in the UK. Geoderma 151, 141–149. https://doi.org/10.1016/j.geoderma.2009.03.021.

Ballantine, D., Walling, D.E., Leeks, G.J.L., 2009b. Mobilisation and transport of sediment-associated phosphorus by surface runoff. Water Air Soil Pollut. 196, 311–320. https://doi.org/10.1007/s11270-008-9778-9.

Barneveld, R.J., van der Zee, S.E.A.T.M., Greipsland, I., Kværnø, S.H., Stolte, J., 2019. Prioritising areas for soil conservation measures in small agricultural catchments in Norway, using a connectivity index. Geoderma 340, 325–336. https://doi.org/10.1016/j.geoderma.2019.01.017.

Bechmann, M., 2014. Long-term monitoring of nitrogen in surface and subsurface runoff from small agricultural dominated catchments in Norway. Agric. Ecosyst. Environ. 198, 13–24. https://doi.org/10.1016/j.agee.2014.05.010.

Bechmann, M., Deelstra, J., Stålnacke, P., Eggestad, H.O., Øygarden, L., Pengerud, A., 2008. Monitoring catchment scale agricultural pollution in Norway: policy instruments, implementation of mitigation methods and trends in nutrient and sediment losses. Environ. Sci. Policy 11, 102–114. https://doi.org/10.1016/j.envsci.2007.10.005.

Beldring, S., Engeland, K., Roald, L.A., Sælthun, N.R., Voksø, A., 2003. Estimation of parameters in a distributed precipitation-runoff model for Norway. Hydrol. Earth Syst. Sci. 7, 304–316. https://doi.org/10.5194/hess-7-304-2003.

Bieroza, M., Bergström, L., Ulén, B., Djodjic, F., Tonderski, K., Heeb, A., Svensson, J., Malgeryd, J., 2019. Hydrologic extremes and legacy sources can override efforts to mitigate nutrient and sediment losses at the catchment Scale. J. Environ. Qual. 48, 1314–1324. https://doi.org/10.2134/jeq2019.02.0063.

Bieroza, M.Z., Heathwaite, A.L., 2015. Seasonal variation in phosphorus concentration-discharge hysteresis inferred from high-frequency in situ monitoring. J. Hydrol. 524, 333–347. https://doi.org/10.1016/j.jhydrol.2015.02.036.

Blankenberg, A.G.B., Skarbøvik, E., 2020. Phosphorus retention, erosion protection and farmers' perceptions of riparian buffer zones with grass and natural vegetation: case studies from South-Eastern Norway. Ambio 49, 1838–1849. https://doi.org/10.1007/s13280-020-01361-5.

Bol, R., Gruau, G., Mellander, P.E., Dupas, R., Bechmann, M., Skarbøvik, E., Bieroza, M., Djodjic, F., Glendell, M., Jordan, P., Van der Grift, B., Rode, M., Smolders, E., Verbeeck, M., Gu, S., Klumpp, E., Pohle, I., Fresne, M., Gascuel-Odoux, C., 2018. Challenges of reducing phosphorus based water eutrophication in the agricultural landscapes of Northwest Europe. Front. Mar. Sci. 5, 1–16. https://doi.org/10.3389/fmars.2018.00276.

Borselli, L., Cassi, P., Torri, D., 2008. Prolegomena to sediment and flow connectivity in the landscape: a GIS and field numerical assessment. CATENA 75, 268–277. https://doi.org/10.1016/j.catena.2008.07.006.

Bracken, L.J., Wainwright, J., Ali, G.A., Tetzlaff, D., Smith, M.W., Reaney, S.M., Roy, A.G., 2013. Concepts of hydrological connectivity: research approaches, pathsways and future agendas. Earth Surf. Process. Landf. 119, 17–34. https://doi.org/10.1063/1.2756072.

Brendel, C.E., Soupir, M.L., Long, L.A.M., Helmers, M.J., Ikenberry, C.D., Kaleita, A.L., 2019. Catchment-scale phosphorus export through surface and drainage pathways. J. Environ. Qual. 48, 117–126. https://doi.org/10.2134/jeq2018.07.0265.

Buck, O., Niyogi, D.K., Townsend, C.R., 2004. Scale-dependence of land use effects on water quality of streams in agricultural catchments. Environ. Pollut. 130, 287–299. https://doi.org/10.1016/j.envpol.2003.10.018.

Cassidy, R., Jordan, P., Bechmann, M., Kronvang, B., Kyllmar, K., Shore, M., 2018. Assessments of composite and discrete sampling approaches for water quality monitoring. Water Resour. Manag. 32, 3103–3118. https://doi.org/10.1007/s11269-018-1978-5.

Casson, N.J., Wilson, H.F., Higgins, S.M., 2019. Hydrological and seasonal controls of phosphorus in Northern Great Plains agricultural streams. J. Environ. Qual. 48, 978–987. https://doi.org/10.2134/jeq2018.07.0281.

Deelstra, J., 2015. Climate change and subsurface drainage design: results from a small field-scale catchment in south-western Norway. Acta Agric. Scand. Sect. B Soil Plant Sci. 65, 58–65. https://doi.org/10.1080/09064710.2014.975836.

Dupas, R., Tavenard, R., Fovet, O., Gilliet, N., Grimaldi, C., Gascuel-Odoux, C., 2015. Identifying seasonal patterns of phosphorus storm dynamics with dynamic time warping. Water Resour. Res. 51, 8868–8882. https://doi.org/10.1002/2015WR017338.Received.

EU, 2000. Water framework directive. Directive 2000/60/EC of the European Parliament and the Council of 23 October 2000 Establishing a Framework for Community Action in the Field of Water Policy.

Evans, C., Davies, T.D., 1998. Causes of concentration/discahrge hysteresis and its potential as a tool for analysis of episode hydrochemistry. Water Resour. Res. 34, 129–137. https://doi.org/10.1029/97WR01881.

Farkas, C., Beldring, S., Bechmann, M., Deelstra, J., 2013. Soil erosion and phosphorus losses under variable land use as simulated by the INCA-P model. Soil Use Manag. 29, 124–137. https://doi.org/10.1111/j.1475-2743.2012.00430.x.

Fovet, O., Humbert, G., Dupas, R., Gascuel-Odoux, C., Gruau, G., Jaffrezic, A., Thelusma, G., Faucheux, M., Gilliet, N., Hamon, Y., Grimaldi, C., 2018. Seasonal variability of stream water quality response to storm events captured using high-frequency and multi-parameter data. J. Hydrol. 559, 282–293. https://doi.org/10.1016/j.jhydrol.2018.02.040.

Gao, H., Shao, M., 2015. Effects of temperature changes on soil hydraulic properties. Soil Tillage Res. 153, 145–154. https://doi.org/10.1016/j.still.2015.05.003.

Gippel, C.J., 1995. Potential of turbidity monitoring for measuring the transport of suspended solids in streams. Hydrol. Process. 9, 83–97. https://doi.org/10.1002/hyp.3360090108.

Giri, S., Qiu, Z., 2016. Understanding the relationship of land uses and water quality in twenty first century: a review. J. Environ. Manag. 173, 41–48. https://doi.org/10.1016/j.jenvman.2016.02.029.

Hanssen-Bauer, I., Førland, E.J., Haddeland, I., Hisdal, H., Mayer, S., Nesje, A., Nilsen, J. E., Sandven, S., Sandø, A., Sorteberg, A., Ådlandsvik, B., 2015. Climate in Norway 2100 - a Knowledge Base for Climate Adaption, Trondheim (in Norwegian, English summary).

Haygarth, P.M., Page, T.J.C., Beven, K.J., Freer, J., Joynes, A., Butler, P., Wood, G.A., Owens, P.N., 2012. Scaling up the phosphorus signal from soil hillslopes to headwater catchments. Freshw. Biol. 57, 7–25. https://doi.org/10.1111/j.1365-2427.2012.02748.x.

Heidel, S.G., 1956. The progressive lag of sediment concentration with flood waves. Eos Trans. Am. Geophys. Union 37, 56–66. https://doi.org/10.1029/TR037i001p00056.

Kämäri, M., Tarvainen, M., Kotamäki, N., Tattari, S., 2020. High-frequency measured turbidity as a surrogate for phosphorus in boreal zone rivers: appropriate options and critical situations. Environ. Monit. Assess. 192 https://doi.org/10.1007/s10661-020-08335-w.

Keesstra, S.D., Davis, J., Masselink, R.H., Casalí, J., Peeters, E.T.H.M., Dijksma, R., 2019. Coupling hysteresis analysis with sediment and hydrological connectivity in three agricultural catchments in Navarre, Spain. J. Soil. Sediment. 19, 1598–1612. https://doi.org/10.1007/s11368-018-02223-0.

Kleinman, P.J.A., Sharpley, A.N., McDowell, R.W., Flaten, D.N., Buda, A.R., Tao, L., Bergstrom, L., Zhu, Q., 2011. Managing agricultural phosphorus for water quality protection: principles for progress. Plant Soil 349, 169–182. https://doi.org/10.1007/s11104-011-0832-9.

Krogstad, T., Øgaard, A.F., 2008. Phosphorus transport in soil profiles by increasing levels of plant available P. Bioforsk Fokus 1 (3), 53 (In Norwegian).

Kværnø, S.H., Øygarden, L., 2006. The influence of freeze-thaw cycles and soil moisture on aggregate stability of three soils in Norway. CATENA 67, 175–182. https://doi.org/10.1016/j.catena.2006.03.011.

Kyllmar, K., Carlsson, C., Gustafson, A., Ulén, B., Johnsson, H., 2006. Nutrient discharge from small agricultural catchments in Sweden. Characterisation and trends. Agric. Ecosyst. Environ. 115, 15–26. https://doi.org/10.1016/j.agee.2005.12.004.

Lannergård, E.E., Ledesma, J.L.J., Fölster, J., Futter, M.N., 2019. An evaluation of high frequency turbidity as a proxy for riverine total phosphorus concentrations. Sci. Total Environ. 651, 103–113. https://doi.org/10.1016/j.scitotenv.2018.09.127.

Lawler, D.M., Petts, G.E., Foster, I.D.L., Harper, S., 2006. Turbidity dynamics during spring storm events in an urban headwater river system: the Upper Tame, West Midlands, UK. Sci. Total Environ. 360, 109–126. https://doi.org/10.1016/j.scitotenv.2005.08.032.

Lefrançois, J., Grimaldi, C., Gascuel-Odoux, C., Gilliet, N., 2007. Suspended sediment and discharge relationships to identify bank degradation as a main sediment source on small agricultural catchments. Hydrol. Process. 21, 2923–2933. https://doi.org/10.1002/hyp.6509.

Leigh, C., Kandanaarachchi, S., McGree, J.M., Hyndman, R.J., Alsibai, O., Mengersen, K., Peterson, E.E., 2019. Predicting sediment and nutrient concentrations from high-frequency water-quality data. PLoS One 14, 1–22. https://doi.org/10.1371/journal.pone.0215503.

Liu, J., Baulch, H.M., Macrae, M.L., Wilson, H.F., Elliott, J.A., Bergström, L., Glenn, A.J., Vadas, P.A., 2019. Agricultural water quality in cold climates: Processes, drivers, management options, and research needs. J. Environ. Qual. 48, 792–802. https://doi.org/10.2134/jeq2019.05.0220.

Luo, J., Zheng, Z., Li, T., He, S., 2018. Assessing the impacts of microtopography on soil erosion under simulated rainfall, using a multifractal approach. Hydrol. Process. 32, 2543–2556. https://doi.org/10.1002/hyp.13170.

Marttila, H., Saarinen, T., Celebi, A., Kløve, B., 2013. Transport of particle-associated elements in two agriculture-dominated boreal river systems. Sci. Total Environ. 461–462, 693–705. https://doi.org/10.1016/j.scitotenv.2013.05.073.

Minella, J.P.G.G., Merten, G.H., Reichert, J.M., Clarke, R.T., 2008. Estimating suspended sediment concetrations from turbidity measurements and the calibration problem. Hydrol. Process. 22, 1819–1830. https://doi.org/10.1002/hyp.6763.

Outram, F.N., Cooper, R.J., Sünnenberg, G., Hiscock, K.M., Lovett, A.A., 2016. Antecedent conditions, hydrological connectivity and anthropogenic inputs: factors affecting nitrate and phosphorus transfers to agricultural headwater streams. Sci. Total Environ. 545–546, 184–199. https://doi.org/10.1016/j.scitotenv.2015.12.025.

Øygarden, L., 2000. Soil Erosion in Small Agricultural Catchments, South Easter Norway (Doctor Scientiarum Theses). Agricultural Uniersity of Norway.

Øygarden, L., 2003. Rill and gully development during an extreme winter runoff event in Norway. CATENA 50, 217–242. https://doi.org/10.1016/S0341-8162(02)00138-8.

Peel, M.C., Finlayson, B.L., McMahon, T.A., 2007. Updated world map of the Köppen-Geiger climate classification. Hydrol. Earth Syst. Sci. 11, 1633–1644. https://doi.org/10.5194/hess-11-1633-2007.

Rankinen, K., Gao, G., Granlund, K., Grönroos, J., Vesikko, L., 2015. Comparison of impacts of human activities and climate change on water quantity and quality in Finnish agricultural catchments. Landsc. Ecol. 30, 415–428. https://doi.org/10.1007/s10980-014-0149-1.

Rose, L.A., Karwan, D.L., Godsey, S.E., 2018. Concentration–discharge relationships describe solute and sediment mobilization, reaction, and transport at event and

longer timescales. Hydrol. Process. 32, 2829–2844. https://doi.org/10.1002/hyp.13235.
Sandström, S., Futter, M.N., Kyllmar, K., Bishop, K., O'Connell, D.W., Djodjic, F., 2020. Particulate phosphorus and suspended solids losses from small agricultural catchments: links to stream and catchment characteristics. Sci. Total Environ. 711, 134616 https://doi.org/10.1016/j.scitotenv.2019.134616.
SeNorge.no, 2020. Data on soil water characteristics. ⟨http://www.senorge.no⟩. (Accessed 10 October 2020).
Schoumans, O.F., Chardon, W.J., Bechmann, M., Gascuel-Odoux, C., Hofman, G., Kronvang, B., Rubæk, G.H., Ulén, B., Dorioz, J.-M., 2014. Mitigation options to reduce phophorus losses from agricultural sector and improve surface water quality: A review. Sci. Total Environ. 468-469, 1255–1266. https://doi.org/10.1016/j.scitotenv.2013.08.061.
Sharpley, A.N., Kleinman, P.J.A., Jordan, P., Bergström, L., Allen, A.L., 2009. Evaluating the success of phosphorus management from field to watershed. J. Environ. Qual. 38, 1981–1988. https://doi.org/10.2134/jeq2008.0056.
Skarbøvik, E., Roseth, R., 2015. Use of sensor data for turbidity, pH and conductivity as an alternative to conventional water quality monitoring in four Norwegian case studies. Acta Agric. Scand. Sect. B Soil Plant Sci. 65, 63–73. https://doi.org/10.1080/09064710.2014.966751.
Skarbøvik, E., Stålnacke, P., Bogen, J., Bønsnes, T.E., 2012. Impact of sampling frequency on mean concentrations and estimated loads of suspended sediment in a Norwegian river: implications for water management. Sci. Total Environ. 433, 462–471. https://doi.org/10.1016/j.scitotenv.2012.06.072.
Skøien, S.E., Børresen, T., Bechmann, M., 2012. Effect of tillage methods on soil erosion in Norway. Acta Agric. Scand. Sect. B Soil Plant Sci. 62, 191–198. https://doi.org/10.1080/09064710.2012.736529.
Stutter, M., Dawson, J.J.C., Glendell, M., Napier, F., Potts, J.M., Sample, J., Vinten, A., Watson, H., 2017. Evaluating the use of in-situ turbidity measurements to quantify fluvial sediment and phosphorus concentrations and fluxes in agricultural streams. Sci. Total Environ. 607–608, 391–402. https://doi.org/10.1016/j.scitotenv.2017.07.013.
Stutter, M., Kronvang, B., Ó hUallacháin, D., Rozemeijer, J., 2019. Current insights into the effectiveness of riparian management, attainment of multiple benefits, and potential technical enhancements. J. Environ. Qual. 48, 236–247. https://doi.org/10.2134/jeq2019.01.0020.
Ulén, B., Aronsson, H., Bechmann, M., Krogstad, T., Øygarden, L., Stenberg, M., 2010. Soil tillage methods to control phosphorus loss and potential side-effects: a Scandinavian review. Soil Use Manag. 26, 94–107.
Ulén, B., Bechmann, M., Fölster, J., Jarvie, H.P., Tunney, H., Folster, J., Bechmann, M., Jarvie, H.P., Tunney, H., Fölster, J., Jarvie, H.P., Tunney, H., 2007. Agriculture as a phosphorus source for eutrophication in the north-west European countries, Norway, Sweden, United Kingdom and Ireland: a review. Soil Use Manag. 23, 5–15. https://doi.org/10.1111/j.1475-2743.2007.00115.x.
Ulén, B., Larsbo, M., Koestel, J., Hellner, Q., Blomberg, M., Geranmayeh, P., 2018. Assessing strategies to mitigate phosphorus leaching from drained clay soils. Ambio 47, 114–123. https://doi.org/10.1007/s13280-017-0991-x.
Valkama, P., Ruth, O., 2017. Impact of calculation method, sampling frequency and Hysteresis on suspended solids and total phosphorus load estimations in cold climate. Hydrol. Res. 48, 1594–1610. https://doi.org/10.2166/nh.2017.199.
Villa, A., Fölster, J., Kyllmar, K., 2019. Determining suspended solids and total phosphorus from turbidity: comparison of high-frequency sampling with conventional monitoring methods. Environ. Monit. Assess. 191, 605. https://doi.org/10.1007/s10661-019-7775-7.
Walling, D.E., Webb, B.W., Russell, M.A., 1997. Sediment-associated nutrient transport in UK rivers. IAHS-AISH Publ. 243, 69–81.
Wenng, H., Bechmann, M., Krogstad, T., Skarbøvik, E., 2020. Climate effects on land management and stream nitrogen concentration in small agricultural catchments in Norway. Ambio 49, 1747–1758. https://doi.org/10.1007/s13280-020-01359-z.
Williams, G.P., 1989. Sediment concentration versus water discharge during single hydrologic events in rivers. J. Hydrol. 111, 89–106. https://doi.org/10.1016/0022-1694(89)90254-0.
Wiréhn, L., 2018. Nordic agriculture under climate change: a systematic review of challenges, opportunities and adaptation strategies for crop production. Land Use Policy 77, 63–74. https://doi.org/10.1016/j.landusepol.2018.04.059.
Withers, P.J.A.A., May, L., Jarvie, H.P., Jordan, P., Doody, D., Foy, R.H., Bechmann, M., Cooksley, S., Dils, R., Deal, N., 2012. Nutrient emissions to water from septic tank systems in rural catchments: uncertainties and implications for policy. Environ. Sci. Policy 24, 71–82. https://doi.org/10.1016/j.envsci.2012.07.023.
Wu, Y., Ouyang, W., Hao, Z., Lin, C., Liu, H., Wang, Y., 2018. Assessment of soil erosion characteristics in response to temperature and precipitation in a freeze-thaw watershed. Geoderma 328, 56–65. https://doi.org/10.1016/j.geoderma.2018.05.007.